Side-Chain Engineering to Optimize the Charge Transport Properties of Isoindigo-based Random Terpolymers for High-Performance Organic Field-Effect Transistors

Yuchang Du[a, b], Hongbing Yao[a, b], Luke Galuska[c], Feng Ge[a], Xiaohong Wang[a, b], Hongbo Lu[a, b], Guobing Zhang[a, b, *], Xiaodan Gu[c, *], and Longzhen Qiu[a, b, *]

[a]National Engineering Lab of Special Display Technology, State Key Lab of Advanced Display Technology, Academy of Opto-Electronic Technology, Hefei University of Technology, Hefei 230009, China

[b]Key Laboratory of Advanced Functional Materials and Devices, Anhui Province, School of Chemistry and Chemical Engineering, Hefei University of Technology, Hefei 230009, China

[c]School of Polymer Science and Engineering, The University of Southern Mississippi, Hattiesburg, MS 39406, USA

E-mail: gbzhang@hfut.edu.cn, xiaodan.gu@usm.edu, lzhqiu@hfut.edu.cn

Abstract:

Random copolymerization is a simple and effective method to regulate and improve the performance of conjugated polymers. Herein, random copolymerization is employed to finely tune the transport behavior of terpolymers by side chain engineering and BIBDF incorporation. Two series of terpolymers have been synthesized by varying the side chain branching positions and BIBDF content. The spectral absorption, electrochemical behavior, microstructure and electrical performance in organic field effect transistors have been systematically studied. The results reveal that the side chain branching points influence the crystallinity, π-π interactions and charge transport behavior of as-prepared terpolymers. Furthermore, the influence of BIBDF content is studied under optimal side chain branching position, which suggests that optical absorption, molecular packing and electrical properties of terpolymers can also be controlled by BIBDF content. For instance, C33P2.5 polymer, with optimal side chain branching position and BIBDF content, exhibited maximum mobility of 7.01 $cm^2 V^{-1} s^{-1}$, which is three times higher than the reference polymer C11P3.75 and C30P0. The current study presents a novel route to maximize the performance of conjugated terpolymers and provides a baseline for further research on high-performance conjugated polymers for a wide array of applications.

Introduction

Conjugated polymers are being extensively studied as active materials in flexible, low-cost and large area optoelectronic devices.[1-7] Carrier mobility is one of the vital performance parameters of conjugated polymers, which is significantly influenced by the chemical structure of the polymer.[8-11] In order to optimize the performance of conjugated polymers, a large number of molecular designs and modification strategies have been developed. In particular, donor-acceptor (D-A) conjugated copolymers, with alternatively amalgamated electron-rich and electron-deficient units, have garnered considerable research attention. [12-16] The modular design of the donor and acceptor moieties in D-A conjugated copolymer can facilitate the fine-tuning of microstructure, electronic and optical properties of organic field-effect transistors (OFETs) and organic photovoltaics (OPV). [17-22] For instance, the utilization of D-A conjugated polymers, as active materials in OFET and OPV devices, resulted in significantly improved charge carrier mobility of 10 cm^2 V^{-1} s^{-1} [23, 24] and power conversion efficiency (PCE) of >10%.[25, 26] However, the design and synthesis of construction units is a challenging task for high-performance D-A polymers because of which needs to have very strict requirements on backbone planarity, electronic structure and solubility. Therefore, the limited monomers leads to inefficiencies in the development of new high performance D-A conjugated polymers.[27, 28]

Recently, the development of random copolymerization enabled the efficient incorporation of a third component into two-component D-A conjugated polymer, which reduces the complexity of building blocks synthesis and effectively tunes the light absorption, energy level and crystallinity of conjugated polymers. [29-32] In general, the introduction of a third component is liable to disturb the planarity and interchain alignment of backbone due to the difference in the structural units during random copolymerization, which results in more amorphous regions and renders inferior carrier mobility. [33, 34] Therefore, it is important to select the structural units which are capable of adjusting the properties without disturbing the ordered packing and even increase locally crystalline regions in conjugated polymers. [30, 32, 35] The donors in D-A conjugated polymers, such as thiophene or selenophene derivatives,

possess similar structure, which allows for maintaining the ordered packing of the polymer backbone during the incorporation of another donor component. For instance, Kim et al. [35] have reported that the random terpolymers not only enhanced the planarity and intermolecular packing of backbone chains but also maintained the inherent characteristics of each polymer. Moreover, the hole and electron mobility of as high as 6.23 and 6.88 $cm^2 V^{-1} s^{-1}$, respectively, can be achieved by precisely adjusting the ratio of two donor monomers. However, the donors with high-lying orbital energy levels limits the range of properties-regulation for random terpolymer. On the other hand, the acceptors are more diverse and render a large regulation range of structures and electronic properties. Hence, the introduction of a second acceptor in random copolymers is a promising route to adjust the absorption spectrum and energy level. [29, 36-42] However, it tend to decrease the planarity and backbone regularity due to the complexity and mismatch of acceptor structure, which is detrimental to carrier transport. Hence, the reports about random terpolymer on acceptor-induced carrier transport enhancement are rare. Recently, we have exploited the structural similarities between isoindigo and its derivative bis (2-oxoindolin-3-ylidene) benzodifurandione (BIBDF) and synthesized BIBDF-containing isoindigo-based polymer by chemical blending. The strong electron-withdrawing BIBDF units enhanced intermolecular π-π interactions and the crystalline structure of the polymer, which led to a remarkable increase in carrier mobility from 0.71 to 2.17 $cm^2 V^{-1} s^{-1}$. [28]

Apart from the backbone structure, the side chains also influence the microstructure and properties of the polymers. It is well known that side chain engineering involves length and branching points, which play a critical role in polymers solubility, solid-state packing of the molecules, thin film morphology and charge transport behavior. [24, 43-52] Therefore, the rational design of side chains is a promising strategy to obtain high-performance solution-processable conjugated polymers. For instance, Pei et al. [44] have demonstrated that adjusting the branching point far away from the conjugated backbone can enhance the carrier mobility of polymers. The results revealed that the larger linear spacer between side chain and backbone reduces π-π stacking distance between intermolecular, which is favorable

for high charge carrier mobility. Even though the influence of side chain engineering on structure, morphology and transport properties of two-component D-A conjugated polymers has been systematically studied, side chain engineering in more complex structure of random terpolymers has received little attention.

Furthermore, the mobility of ID-based polymers has been significantly improved by simple random copolymerization of a third unit, i.e., BIBDF. [28] However, the influence of both side and main chains on terpolymer properties remains unclear and requires a comprehensive investigation. Herein, two series of polymers have been synthesized by systematically varying the branching position in side chain and BIBDF content in the main chain (Schematic 1). The electrical performance of as-synthesized polymers has been characterized in bottom-gate/top-contact (BGTC) field-effect transistors under surrounding conditions. In addition, the microstructure and morphological features of as-prepared polymers have been investigated by using grazing incident wide-angle X-ray scattering (GIWAXS) and tapping-mode atomic force microscopy (AFM). The results reveal that side chain branching position remarkably influenced the crystallinity of as-synthesized polymeric films and reduced π-π stacking distance between intermolecular. Moreover, the optimal BIBDF content also enhanced the crystallinity and altered π-π interactions in as-synthesized polymers. Among all the as-prepared polymers, the terpolymer C33P2.5 exhibited maximum mobility of 7.01 $cm^2 V^{-1} s^{-1}$ and a high I_{on}/I_{off} ratio of 10^7.

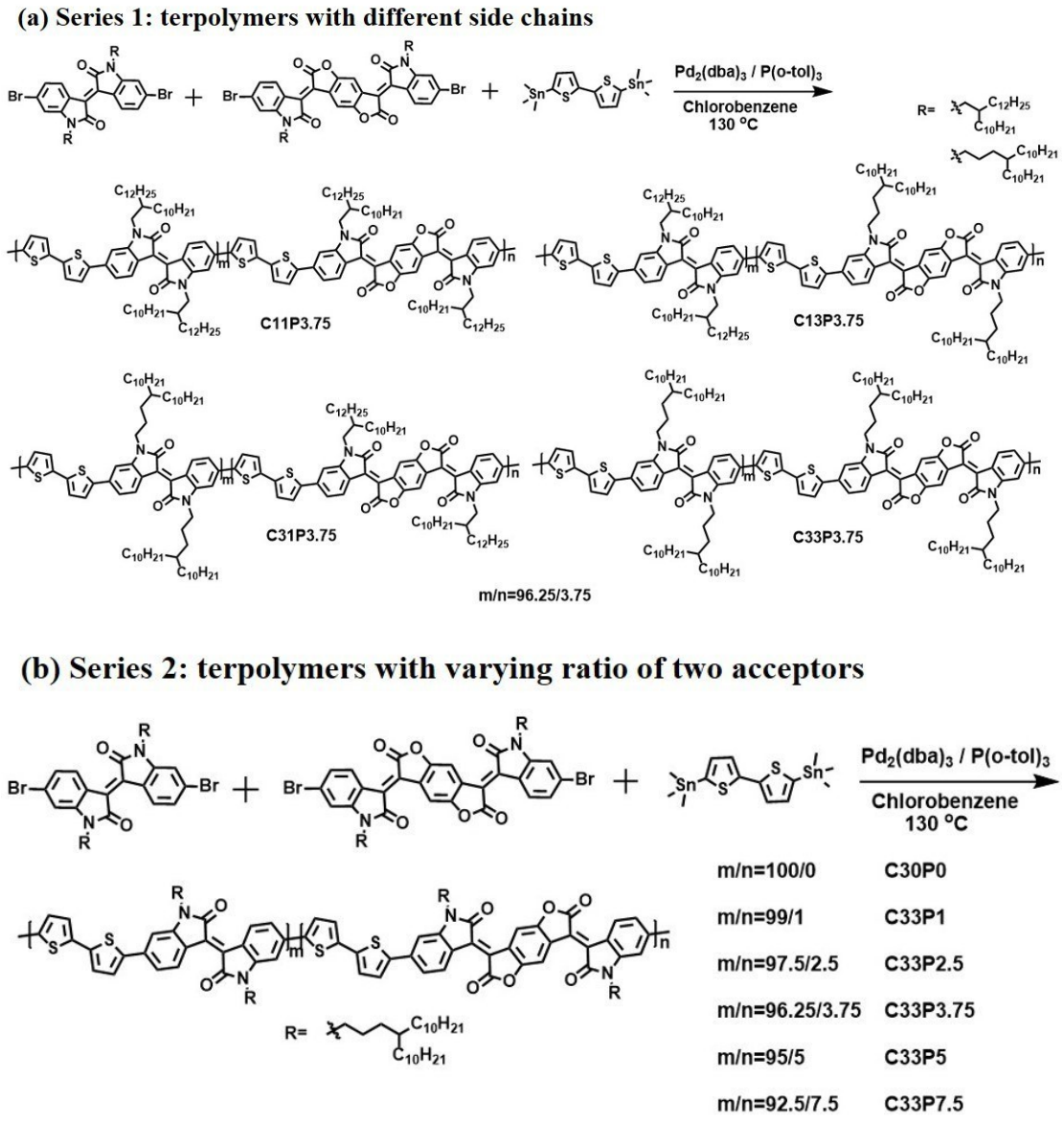

Schematic 1. Synthesis scheme and chemical structure of random terpolymers.

Table 1. Optical and electrochemical properties of polymers with different side chains.

polymers	Mn [kDa] / PDI	Td [°C]	$\lambda_{max}^{solu.}$ [nm]	λ_{max}^{film} [nm]	λ_{onset} [nm]	E_g^{opt} [eV]	E_{HOMO} [eV]	E_{LUMO} [eV]	E_g^{CV} [eV]
C11P3.75	33.9/4.0	384	709	706	850	1.46	-5.59	-3.62	1.97
C13P3.75	29.6/3.9	382	708	705	857	1.45	-5.60	-3.62	1.98
C31P3.75	46.0/3.3	389	716	719	860	1.44	-5.49	-3.63	1.86
C33P3.75	42.9/3.4	394	717	720	860	1.44	-5.47	-3.61	1.86

Table 2. Optical and electrochemical properties of polymers with different BIBDF contents.

polymers	Mn [kDa] / PDI	Td [°C]	$\lambda_{max}^{solu.}$ [nm]	λ_{max}^{film} [nm]	λ_{onset} [nm]	E_g^{opt} [eV]	E_{HOMO} [eV]	E_{LUMO} [eV]	E_g^{CV} [eV]	E_{HOMO} [UPS] [eV]
C30P0	45.7/3.1	398	719	718	788	1.57	-5.45	-3.57	1.88	-5.62
C33P1	45.1/3.2	394	718	720	803	1.54	-5.48	-3.60	1.88	-5.73
C33P2.5	51.0/2.9	393	717	720	816	1.52	-5.46	-3.61	1.85	-5.69
C33P3.75	42.9/3.4	394	717	720	860	1.44	-5.47	-3.61	1.86	-5.66
C33P5	42.8/3.5	399	716	719	865	1.43	-5.47	-3.62	1.85	-5.63
C33P7.5	39.0/3.7	393	714	719	887	1.40	-5.47	-3.63	1.84	-5.60

RESULTS AND DISCUSSION

Schematic 1 presents two series of as-synthesized random terpolymers, where one possesses the same acceptors ratio and different side chains and the other contains different acceptors ratio at optimized side chains. The monomers, such as 6,6'-Dibromodi(2-decyltetradecyl)isoindigo (2Br-ID-C1), [53] 6,6'-Dibromodi(4-decyltetradecyl)isoindigo (2Br-ID-C3), [44] (3E,7E)-3,7-bis(6-bromo-1-(2-decyltetradecyl)-2-oxoindolin-3-ylidene)benzo[1,2-b:4,5-b']difuran-2,6(3H,7H)-dione (2Br-BIBDF-C1), [54, 55] (3E,7E)-3,7-bis(6-bromo-1-(4-decyltetradecyl)-2-oxoindolin-3-ylidene)benzo[1,2-b:4,5-b']difuran-2,6(3H,7H)-dione (2Br-BIBDF-C3) [56] and 5,5'-bis(trimethylstannyl)-2,2'-dithiophene (DT), [57] have been synthesized by using the previously reported methods. Stille coupling copolymerization of 5,5'-bis(trimethylstannyl)-2,2'-dithiophene with a mixture of 2Br-ID-Cx and 2Br-BIBDF-Cy in different molar proportions produced random terpolymers, which are named as $C_{xy}P_n$, where x and y refer to the linear spacer carbon numbers between side chain branching position and polymer main chain and *n* represents the molar proportion of BIBDF. The reference polymer, designated as C30P0, has also been prepared, as reported elsewhere. [44] The detailed experimental procedure is included in supporting information (SI). Once polymerization is completed, methanol was added to the system to precipitate the as-synthesized polymers, followed by sequential Soxhlet extraction by using acetone, hexane, dichloromethane and chloroform, which

resulted in dark-blue solid flakes. The number-average molecular weight (M_n) of random terpolymers was evaluated by using gel permeation chromatography (GPC), at 100 ° C, with trichlorobenzene as the eluent. The M_n of as-synthesized terpolymers ranged from 29.6 to 51.0 kDa with a polydispersity (PDI) of 2.9-4.0 (Table 1 and 2). Moreover, thermogravimetric analysis (TGA) shows that the decomposition temperature, corresponding to the weight loss of 5%, of the as-synthesized terpolymers is higher than 380 °C (Figure S1). These results indicate that the as-prepared terpolymers exhibit sufficient thermal stability for electronic devices, such as organic thin film transistors.

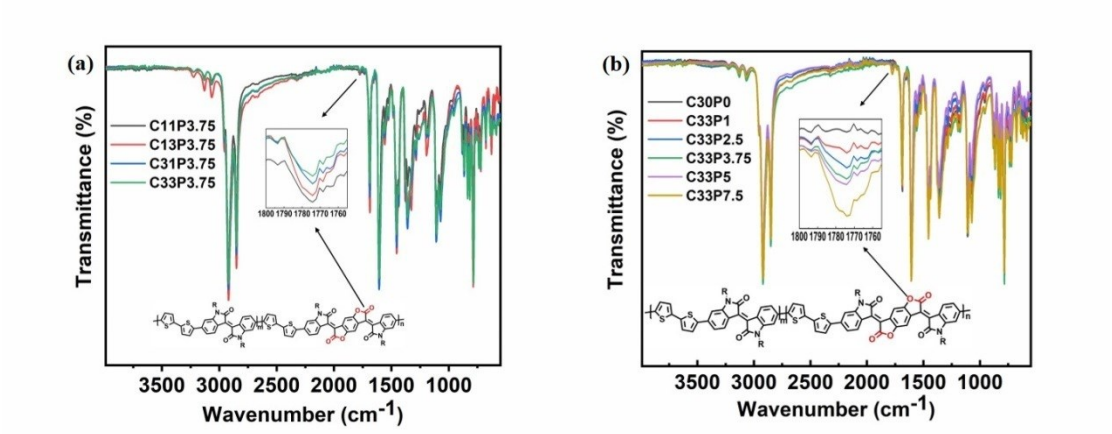

Figure 1. Fourier transform infrared (FTIR) spectra of as-synthesized terpolymers.

The characteristic absorption peaks of as-prepared terpolymers were analyzed by Fourier transform infrared spectroscopy (FTIR). Fig. 1a presents that the typical stretching vibration absorption peak of the five-membered ring lactone, at ~1770 cm^{-1}, possesses similar intensity due to the same amount of BIBDF in C11P3.75 to C33P3.75 polymers. In Series 2, the intensity of the characteristic peak (~1770 cm^{-1}) increased with increasing BIBDF content in C33P1 to C33P7.5 polymers, as shown in Fig. 1b. Moreover, the elemental analysis was carried out to assess the composition of as-prepared random terpolymers (SI).

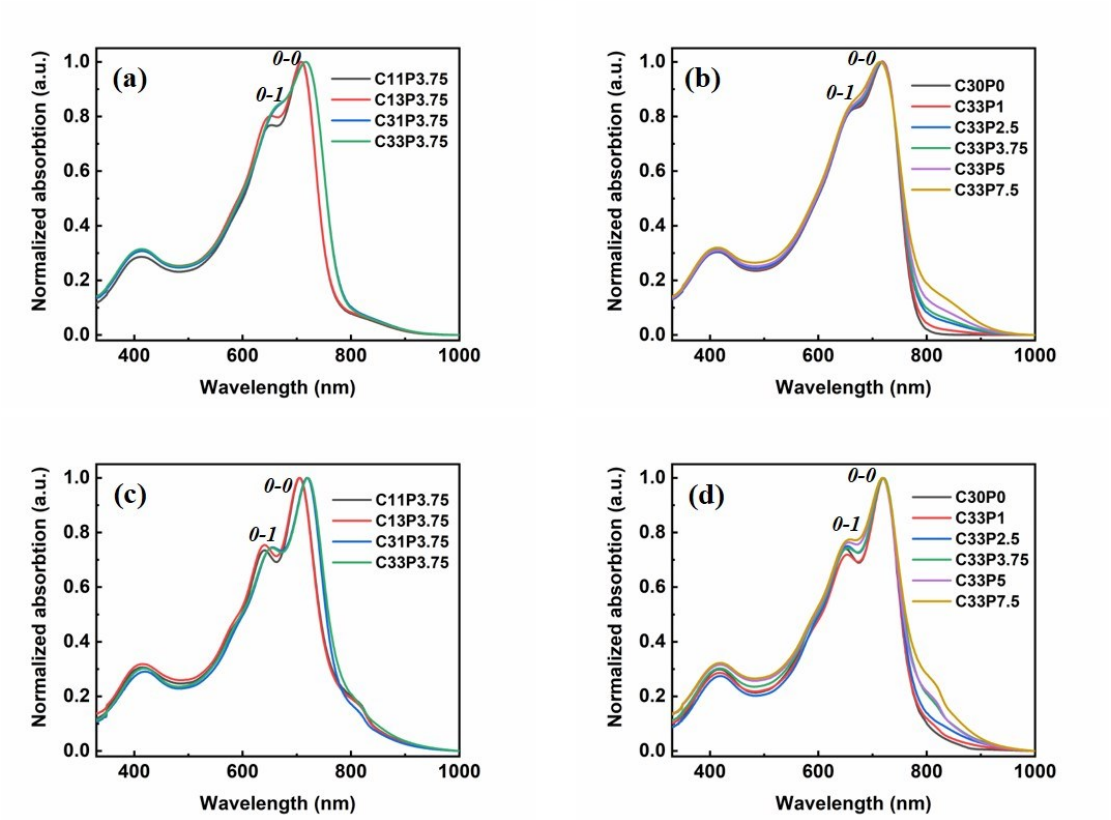

Figure 2. Normalized UV-vis absorption spectra of the random terpolymers in (a-b) $CHCl_3$ solution (1×10^{-5} M) and (c-d) thin films.

Optical and electrochemical characterization:

The UV−vis−NIR absorption spectra of the random terpolymers in chloroform solutions and thin films are presented in Figure 2 and corresponding data are summarized in Table 1-2. In Series 1, C31P3.75 and C33P3.75 have exhibited red-shifted absorption in both solution and thin films compared with C11P3.75 and C13P3.75 terpolymers, which can be attributed to the extending alkyl chain spacer of the side chain on the main acceptor component of isoindigo. The long alkyl spacers in the polymers can reduce steric hindrance and make the main chain of C31P3.75 and C33P3.75 polymers more planar and favorable for intermolecular π-π stacking.[44] The dual shoulder bands, located at ~600-750 nm, correspond to 0-0 and 0-1 vibrational transitions. The difference in intensity suggests that the terpolymers have different pre-aggregation states in solution. As shown in Fig. 2c, C33P3.75, with a longer alkyl spacer on both ID and BIBDF, exhibits the maximum red-shifted absorption in thin film, which indicates the highest planarity and optimal solid-state packing. Moreover,

the absorption peak at ~820 nm for C11P3.75 to C33P3.75 terpolymers can be ascribed to intramolecular charge transfer (ICT) transition from DT to BIBDF unit.

In Series 2, the C30P0 reference and five as-synthesized terpolymers (C33P1-C33P7.5) exhibited two typical absorption bands in both solution and thin film (Figure 2b and 2d). The absorption bands at 350-500 nm and 500-800 nm correspond to π-π* transitions and ICT transition from DT to the ID unit, respectively. The dual shoulder band, corresponding to 0-0 and 0-1 vibrational transitions, indicates some pre-aggregated states of polymers in solution. Compared with absorption bands in solution, the 0-1 transition decreased in thin film, which suggests that polymer backbone become more planar in thin film. Figure 2d presents that the intensity of 0-1 peak first decreased, followed by a gradual increase with increasing BIBDF content, which confirms that the proper ratio of BIBDF can increase the planarity and interaction of the polymer and enhance the electron delocalization. [34, 58] When the BIBDF content was in the range of 1 to 2.5 mol %, the absorption bands of C33P1 and C33P2.5 polymers remained similar to the C30P0 film. However, when the BIBDF content was further increased above 3.75 mol %, the other three terpolymers (C33P3.75-C33P7.5) exhibited a high-intensity peak at ~820 nm, corresponding to the characteristic ICT band from DT to BIBDF. These results indicate that the incorporation of lower BIBDF content (< 2.5 mol %) into ID-based polymer does not interfere with the conjugated structure and regularity of polymeric backbone, but further addition of BIBDF alters the absorption behavior of terpolymers. In addition, as the BIBDF content increased from 1 to 7.5 mol%, the intensity of ICT peaks (~820 nm) gradually increased and the optical bandgap decreased from 1.57 to 1.40 eV.

The electronic energy levels of as-prepared terpolymers thin films were investigated by using cyclic voltammetry (CV). The CV curves are presented in Figure S2 and the corresponding data are summarized in Table 1 and 2. The highest occupied molecular orbital (HOMO) and lowest unoccupied molecular orbital (LUMO) energy levels were calculated by using the given equation:

$$E_{FMO} = -(E_{oneset} + 4.75 \text{ eV})$$

In Series 1, as the branching points of the side chains on the ID or BIBDF are far from

the polymeric backbone, the HOMO energy level gradually increased from -3.60 eV to -3.47 eV for C11P3.75 to C33P3.75 terpolymers, respectively. It can be ascribed to more planar polymer backbones and closer packing due to a significant reduction in steric hindrance. The approximate LUMO levels of these terpolymers indicate that the branching position of side chain has little influence on the LUMO level.

In Series 2, when BIBDF content was increased from 0 to 7.5 mol %, the HOMO and LUMO energy levels decreased from -5.45/-3.57 eV to -5.48 eV/-3.63 eV, respectively, which can be attributed to the strong electron-withdrawing ability of BIBDF acceptor. The electrochemical band gap of as-synthesized terpolymers became narrower due to the introduction of BIBDF, which is consistent with the optical results. Furthermore, ultraviolet photoelectron spectroscopy (UPS) (Figure S3) was carried out to determine the HOMO energy levels of Series 2 terpolymers and investigate the impact of BIBDF on HOMO energy levels. The ionization potentials (IPs) of the as-prepared terpolymers C30P0-C33P7.5 are -5.62, -5.73, -5.69, -5.66, -5.63, -5.60 eV, respectively. One should note that the IPs initially decreased with increasing BIBDF content, followed by a gradual increase, which is consistent with the change in 0-1 absorption intensity, as shown in Figure 2d.

Characterization of organic field effect transistors:

The electrical performance of as-prepared terpolymers was investigated by using a bottom gate/top contact (BGTC) OFET device and the influence of side chain branching position and BIBDF content on carrier mobility of the as-prepared polymers has also been evaluated. The detailed fabrication procedure of OFETs is outlined in SI. These devices are characterized under ambient conditions. The as-prepared terpolymers have exhibited typical p-type transporting behavior. The representative transfer and output curves are presented in Figure 3 and Figure S4, respectively, whereas the corresponding performance parameters are summarized in Table 3-4 and Table S1-S2. In Series 1, as the branching position of the side chains moved away from the backbone of as-prepared random terpolymers, i.e., C11, C13,

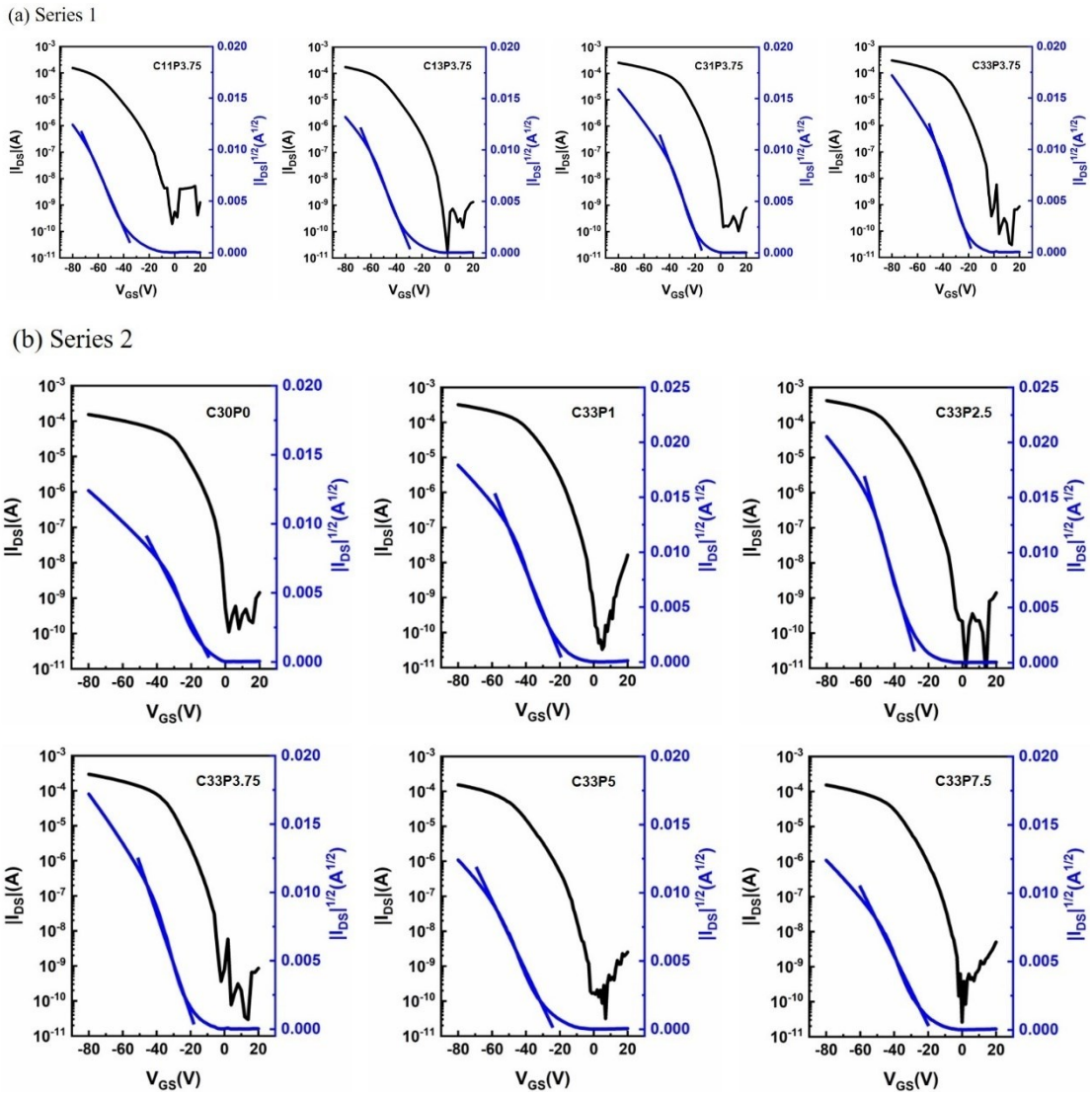

Figure 3. Transfer curves of OFETs of the as-prepared terpolymers (a) with different side chains and (b) different BIBDF ratios after thermal annealing at optimized temperatures.

C31 and C33, the carrier mobility gradually increased (Table S1). Moreover, thermal annealing, at different temperatures, improved the hole mobility of four polymers compared to the respective un-annealed films, which can be ascribed to the enhanced ordered packing due to heat treatment. The maximum carrier mobility of 4.00 cm^2 V^{-1} s^{-1} has been demonstrated by C33P3.75 polymer after thermal annealing at 260 ° C (Table 3 and S1). Similarly, the carrier mobility of the other three polymers, i.e., C11P3.75, C13P3.75 and C31P3.75, increased with annealing temperature and the maximum mobility has been achieved after annealing at 260 ° C. It is worth noting

Table 3. Optimized OFETs performance of terpolymers with different side chains.

Polymer	$\mu_{h, max}$ ($cm^2 V^{-1} s^{-1}$)	$\mu_{h, avg}$ ($cm^2 V^{-1} s^{-1}$)	I_{on} / I_{off}	V_{th} (V)
C11P3.75	2.19	1.89	10^5-10^6	-37.8
C13P3.75	2.44	2.08	10^6-10^7	-31.4
C31P3.75	3.16	2.65	10^6-10^7	-16.8
C33P3.75	4.00	3.66	10^6-10^7	-19.9

Table 4. Optimized OFETs performances of terpolymers with different BIBDF contents.

Polymer	$\mu_{h, max}$ ($cm^2 V^{-1} s^{-1}$)	$\mu_{h, avg}$ ($cm^2 V^{-1} s^{-1}$)	I_{on} / I_{off}	V_{th} (V)
C30P0	2.10	2.05	10^6-10^7	-13.7
C33P1	4.21	4.09	10^6-10^7	-21.8
C33P2.5	7.01	6.01	10^7-10^8	-28.7
C33P3.75	4.00	3.66	10^6-10^7	-19.9
C33P5	1.90	1.65	10^6-10^7	-27.9
C33P7.5	2.00	1.92	10^6-10^7	-23.3

that the absorption bands have exhibited the red-shift and the HOMO level increased as the branching position of side chain moved far away from the polymeric backbone, which can be ascribed to the enhanced planarity and improved π-π stacking of the polymeric backbone.[44] Hence, the results of carrier mobility are consistent with the optical absorption behavior and change in energy levels. The results reveal that subtle

changes in the side chain branching sites remarkably influence the transport properties of the conjugated terpolymer.

In Series 2, the carrier mobility of as-cast devices of six polymers were all exceeded 1.00 $cm^2\ V^{-1}\ s^{-1}$ (Table S2). After annealing at different temperatures, ranging from 180 to 290° C, C30P0 demonstrated maximum mobility after annealing at 180 ° C, C33P1, C33P2.5 and C33P3.75 after annealing at 260° C and C33P5 and C33P7.5 after annealing at 210° C. At the optimum annealing temperature, the maximum and average mobilities for Series 2 polymers (C30P0 to C33P7.5) initially increased with increasing BIBDF, followed by a gradual decrease. Herein, C33P2.5 has exhibited maximum mobility of 7.01 $cm^2\ V^{-1}\ s^{-1}$, an average value of 6.01 $cm^2\ V^{-1}\ s^{-1}$ and a high I_{on}/I_{off} ratio of $>10^7$ (Table 4 and S2). The reference polymer (C30P0) has shown maximum mobility of 2.10 $cm^2\ V^{-1}\ s^{-1}$, which is relatively lower than the previously reported value (3.62 $cm^2\ V^{-1}\ s^{-1}$).[44] This may be due to the differences in device fabrication conditions, such as solvent concentration and surface modifications, etc. However, one should note that the mobility of the as-prepared terpolymer has been significantly improved by introducing a small amount of BIBDF (< 3.75 mol %).[28] Moreover, when BIBDF content was increased to 2.5 mol %, the carrier mobility reached its highest value. However, when the BIBDF content exceeded 5 mol %, the mobility of as-prepared terpolymers became lower than the C30P0 reference polymer.

Table 3 and Table S1 show that the mobility of C33P3.75 (4.00 $cm^2\ V^{-1}\ s^{-1}$) is almost two times higher than C11P3.75 (2.19 $cm^2\ V^{-1}\ s^{-1}$), which is equivalent to the previously reported terpolymer P3.75. [28] Furthermore, Table 4 and Table S2 present that optimal side chain branching position and BIBDF content render maximum mobility of C33P2.5, which is three times higher than the C30P0 reference polymer. These results confirm that both side chain branching position and BIBDF content have a great influence on carried mobility of terpolymers. First, extending the branching position (from C11 to C33) on the side chains of the ID and BIBDF acceptors in random terpolymers enhanced the performance of as-prepared terpolymers. Second, the introduction of only 2.5 mol % BIBDF into C30P0

remarkably improved the carrier mobility of as-prepared terpolymers. Third, when BIBDF content exceeded the threshold limit, the carrier mobility gradually decreased, but terpolymers with a long alkyl spacer (C33) maintained high carrier mobility (~ 2.00 $cm^2 V^{-1} s^{-1}$).

Microstructural Analysis of Polymeric Films

Furthermore, grazing incident wide-angle X-ray scattering (GIWAXS) and tapping-mode atomic force microscopy (AFM) were used to investigate the solid-state packing and influence of the side chain branching sites and BIBDF content on the morphology of polymeric thin films. The samples for microstructural investigation were prepared under the same condition as OFETs. Two-dimensional (2D) GIWAXS patterns and 1D scattering profiles of the polymeric thin films are presented in Figure 4-5 and Figure S5-6. The extracted and calculated data are summarized in Table S3 and S4.

In Series 1, as the branching point extended, the number of diffraction peaks for four unannealed thin films gradually increased along q_z axis in the out-of-plane direction. After annealing at the optimum temperature, the intensity and order of diffraction peaks of four terpolymers have obviously increased. Among them, C33P3.75 has shown the strongest five diffraction peaks along q_z axis, indicating

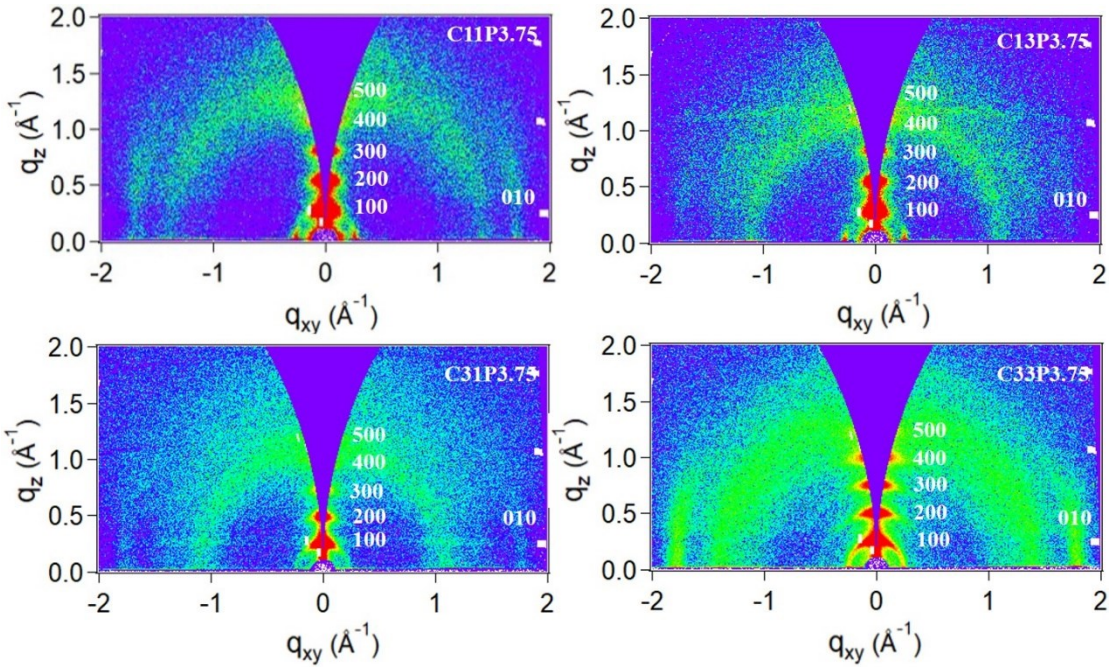

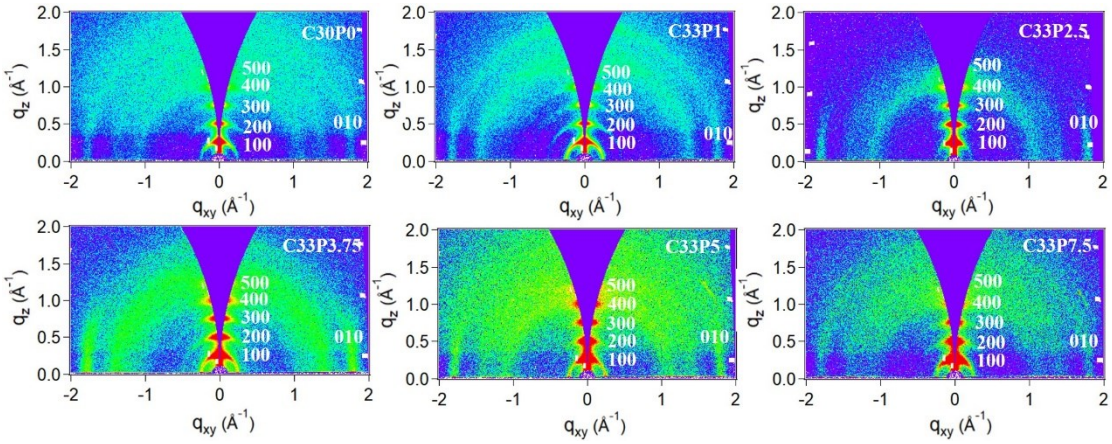

Figure 4. 2D-GIWAXS patterns of polymers with different side chains (top) and different BIBDF content (bottom) after thermal annealing at optimized temperatures.

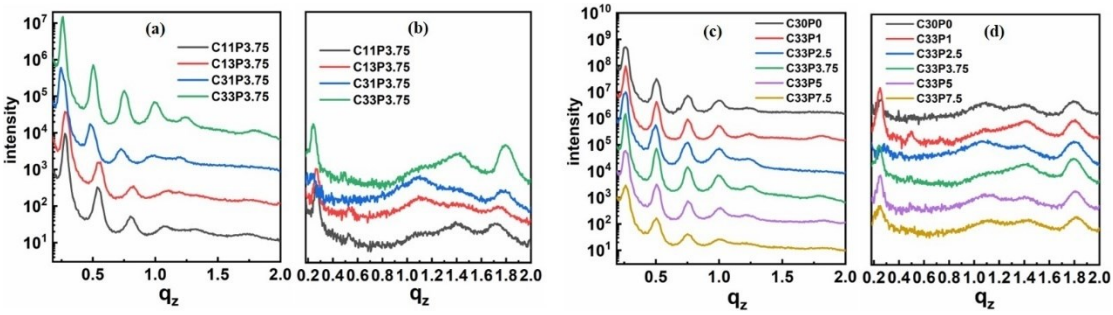

Figure 5. (a, c) Out-of-plane and (b, d) in-plane one-dimensional GIWAXS patterns of as-synthesized terpolymers after thermal annealing at optimized temperatures.

long-range ordered edge-on molecular packing. These results indicate that the extension of branching position in side chains of ID and BIBDF promotes lamellar packing of random terpolymers. In addition, C33P3.75 thin film exhibited a more ordered lamellar structure than the other terpolymers before and after thermal annealing. The lamellar distances are 22.68, 22.05, 24.54 and 24.07 Å for C11P3.75, C13P3.75, C31P3.75 and C33P3.75, respectively. However, the d-spacings of the four polymers did not exhibit any particular trend, which may result from different conformations of the side chains in the film.[47] In addition, the as-synthesized terpolymer thin films exhibited distinct (010) diffraction peaks along q_{xy} axis in the in-plane direction, which indicates the formation of ordered π-π stacking. In as-cast thin films, the intensity of diffraction peaks for C31P3.75 and C33P3.75 polymers are stronger than C11P3.75 and C13P3.75 polymers, which indicates that the ordered

stacking in C3yP3.75 is higher than C1yP3.75. After thermal annealing, the intensity of all (010) diffraction peaks increased. In particular, the diffraction peak for C33P3.75 became sharper and stronger than other polymers. As the extension of the branching position on side chains increased, the π-π stacking distance gradually decreased. The as-prepared C11P3.75, C13P3.75, C31P3.75 and C33P3.75 polymers have exhibited π-π stacking distance of 3.67, 3.60, 3.54 and 3.50 Å, respectively. The out-of-plane and in-plane results suggest that moving the branching site of side chains away from the main chain can not only enhance ordered lamellar packing but also facilitate the closer π-π stacking. These features are beneficial for achieving higher mobility.

In Series 2, the as-cast thin films exhibited distinct and relatively broad out-of-plane (*h*00) diffraction peaks, corresponding to the edge-on lamellar stacking. After annealing at optimized temperature, the out-of-plane (*h*00) diffraction peaks of as-prepared terpolymer films became sharper and stronger than the as-cast films, which indicates the formation of more ordered lamellar packing. Figure 4 and Figure S5 present that, owing to the addition of 1-5 mol % of BIBDF, C33P1 to C33P5 polymers have exhibited five distinct diffraction peaks along q_z axis, which implies that the edge-on lamellar stacking has been enhanced compared to C30P0. This indicates that the incorporation of a proper amount of BIBDF can enhance the regularity of interlamellar packing of the polymers. However, when BIBDF content was increased from 3.75 to 7.5 mol %, the intensity of diffraction peaks gradually decreased, which corresponds to the structural disorder caused by excess BIBDF in the polymer backbone and, in turn, influences the long-range ordered packing of the polymer. The interlayer spacing of all six random terpolymers was approximately 24 Å due to the same side chains. The (010) diffraction peaks, corresponding to π-π stacking, can also be observed in the in-plane direction of six polymer films before and after thermal annealing. Moreover, the intensity of diffraction peaks increased after thermal annealing. When BIBDF content was increased from 0 to 3.75 mol %, the intensities of C33P1-C33P3.75peaks became sharper due to enhanced π-π stacking and improved film crystallinity. However, after a threshold level of BIBDF (above

3.75 mol %), the intensity of C33P5 and C33P7.5 peaks gradually decreased, which indicates that an excessive amount of BIBDF disturbed the ordered structure of the film. The π-π stacking distance of the annealed C33P0, C33P1, C33P2.5, C33P3.75, C33P5 and C33P7.5 films were found to be 3.51, 3.49, 3.47, 3.50, 3.48 and 3.48 Å, respectively. Clearly, the π-π stacking distance became smaller than the reference polymer C30P0 after chemical blending with BIBDF. It is worth noting that C33P2.5 has exhibited the smallest π-π stacking distance among all as-prepared terpolymers. Overall, an optimal amount of BIBDF (< 3.75 mol %) can improve the well-ordered lamellar packing and render closed π-π stacking crystal structure in the polymer films, which effectively improves the transport of charge carriers.

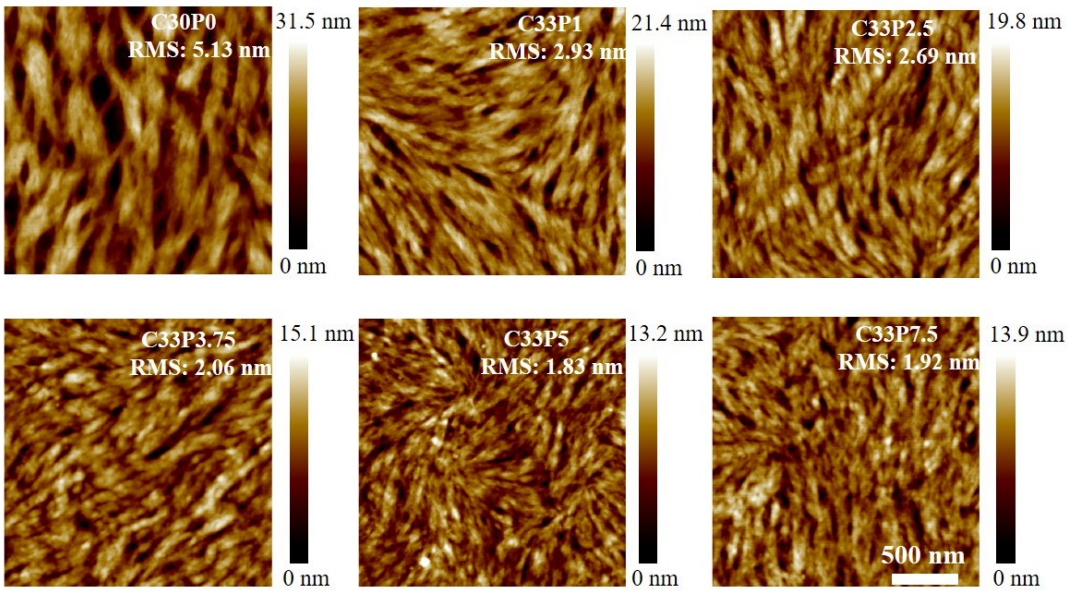

Figure 6. AFM height images of polymer thin films with different BIBDF amounts after thermal annealing at optimized temperatures.

AFM height images of annealed terpolymers films are presented in Figure 6 and S6. As the branching point of side chains moved far from backbone for C11P3.75-C33P3.75 polymers, the surface morphology of polymeric films changed from fine nanowires to wide nanofiber network structure, which indicates an increase in crystallinity and ordered arrangement of the polymer thin films. The C11P3.75 film exhibited interconnected fine-fiber nanostructure, whereas C33P3.75 exhibited the large crystalline domains with fewer grain boundaries, which are beneficial for charge

transport.[59] In Series 2, the reference polymer C30P0 has exhibited oversized fibrillar intercalating networks and macropores, which may be detrimental to carrier transport. [47] Compared with C30P0, C33P1, C33P2.5 and C33P3.75 polymers have shown a relatively uniform and moderate nanofiber-like connective domains. These results demonstrate that three polymers are prone to form crystallites and ordered packing in films, which is highly desirable for excellent charge transport properties.[44] Moreover, C33P5 and C33P7.5 films have shown fine-grained nanofibers with a smooth surface, which indicates that these polymers possess poor crystallinity. These observations are consistent with GIWAX analysis.

Conclusions

In summary, we have demonstrated that fine-tuning of side chain and BIBDF content remarkably influence the transport behavior of ID-based polymers. Two series of random terpolymers have been designed and synthesized by ternary copolymerization. When the branching points of side chains moved away from polymeric backbone, the mobility has shown a remarkable increase and C33P3.75 terpolymer exhibited a carrier mobility of 4 cm^2 V^{-1} s^{-1}. Under the optimized side chain positions, the influence of BIBDF content on transport properties, structure and morphology of as-synthesized terpolymers has been studied. The transport performance of as-prepared terpolymers initially enhanced with increasing BIBDF content, followed by a gradual decrease. The as-prepared terpolymer C33P2.5, with optimal branching position of side chains and BIBDF content, has shown the highest carrier mobility of 7.01 cm^2 V^{-1} s^{-1}, which is almost three times higher than reference polymer C30P0 and C11P3.75. The microstructural investigations demonstrate that i) as the side chain branching points moved far away from the backbone, the lamella packing of the terpolymer films became more ordered and π-π stacking became closer. ii) The molecular packing increased with increasing BIBDF content up to a threshold limit (3.75 mol %). In brief, the performance of conjugated polymer is greatly improved by comprehensively tuning the branching position in side chain and BIBDF content in main chain structure. These results provide a baseline for future work on the design and synthesis of high-performance random terpolymers.

Acknowledgments

This study was supported by National Natural Science Foundation of China (NSFC, 51573036, 51703047), the Distinguished Youth Foundation of Anhui Province (1808085J03), and the Fundamental Research Funds for the Central Universities (JZ2018HGPB0276). L.G and X.G thank financial support from NSF NRT program #1449999 and EPSCOR 8006123 RFA1.

1. Yan, H.; Chen, Z.; Zheng, Y.; Newman, C.; Quinn, J. R.; Dotz, F.; Kastler, M.; Facchetti, A., A high-mobility electron-transporting polymer for printed transistors. *Nature* **2009,** *457* (7230), 679-686.

2. Heeger, A. J., Semiconducting polymers: the Third Generation. *Chem. Soc. Rev.* **2010,** *39* (7), 2354-2371.

3. Sirringhaus, H., 25th anniversary article: organic field-effect transistors: the path beyond amorphous silicon. *Adv Mater* **2014,** *26* (9), 1319-1335.

4. Ostroverkhova, O., Organic Optoelectronic Materials: Mechanisms and Applications. *Chemical reviews* **2016,** *116* (22), 13279-13412.

5. Sokolov, A. N.; Tee, B.C.; Bettinger, C. J.; Tok, J. B.; Bao, Z. N., Chemical and Engineering Approaches To Enable Organic Field-Effect Transistors for Electronic Skin Applications. *Acc. Chem. Res.* **2012,** *45* (3), 361-371.

6. Zang, Y.; Zhang, F.; Huang, D.; Gao, X.; Di, C. A.; Zhu, D., Flexible suspended gate organic thin-film transistors for ultra-sensitive pressure detection. *Nature communications* **2015,** *6*, 6269.

7. Liu, X.; Guo, Y.; Ma, Y.; Chen, H.; Mao, Z.; Wang, H.; Yu, G.; Liu, Y., Flexible, low-voltage and high-performance polymer thin-film transistors and their application in photo/thermal detectors. *Adv Mater* **2014,** *26* (22), 3631-3636.

8. Wang, C.; Dong, H.; Hu, W.; Liu, Y.; Zhu, D., Semiconducting π-conjugated systems in field-effect transistors: a material odyssey of organic electronics. *Chemical reviews* **2012,** *112* (4), 2208-2267.

9. Shuai, Z.; Geng, H.; Xu, W.; Liao, Y.; Andre, J. M., From charge transport parameters to charge mobility in organic semiconductors through multiscale

simulation. *Chem Soc Rev* **2014,** *43* (8), 2662-2679.

10. Coropceanu,V.; Cornil, J.; Filho, D. A. S.; Olivier, Y.; Silbey, R.; Bre´das, J. L., Charge Transport in Organic Semiconductors. *Chem. Rev.* **2007,** *107*, 926-952.

11. Noriega, R.; Rivnay, J.; Vandewal, K.; Koch, F. P.; Stingelin, N.; Smith, P.; Toney, M. F.; Salleo, A., A general relationship between disorder, aggregation and charge transport in conjugated polymers. *Nature materials* **2013,** *12* (11), 1038-1044.

12. Gao, X.; Zhao, Z., High mobility organic semiconductors for field-effect transistors. *Science China-Chemistry* **2015,** *58* (6), 947-968.

13. Guo, X.; Facchetti, A.; Marks, T. J., Imide- and amide-functionalized polymer semiconductors. *Chemical reviews* **2014,** *114* (18), 8943-9021.

14. Yi, Z.; Wang, S.; Liu, Y., Design of High-Mobility Diketopyrrolopyrrole-Based π-Conjugated Copolymers for Organic Thin-Film Transistors. *Adv Mater* **2015,** *27* (24), 3589-3606.

15. Lei, T.; Wang, J. Y.; Pei, J., Design, synthesis, and structure-property relationships of isoindigo-based conjugated polymers. *Accounts of chemical research* **2014,** *47* (4), 1117-1126.

16. Huang, H.; Yang, L.; Facchetti, A.; Marks, T. J., Organic and Polymeric Semiconductors Enhanced by Noncovalent Conformational Locks. *Chemical reviews* **2017,** *117* (15), 10291-10318.

17. Zhang, G.; Zhao, J.; Chow, P. C. Y.; Jiang, K.; Zhang, J.; Zhu, Z.; Zhang, J.; Huang, F.; Yan, H., Nonfullerene Acceptor Molecules for Bulk Heterojunction Organic Solar Cells. *Chemical reviews* **2018,** *118* (7), 3447-3507.

18. Gao, Y.; Deng, Y.; Tian, H.; Zhang, J.; Yan, D.; Geng, Y.; Wang, F., Multifluorination toward High-Mobility Ambipolar and Unipolar n-Type Donor-Acceptor Conjugated Polymers Based on Isoindigo. *Adv Mater* **2017,** *29* (13).

19. Yang, J.; Zhao, Z.; Geng, H.; Cheng, C.; Chen, J.; Sun, Y.; Shi, L.; Yi, Y.; Shuai, Z.; Guo, Y.; Wang, S.; Liu, Y., Isoindigo-Based Polymers with Small Effective Masses for High-Mobility Ambipolar Field-Effect Transistors. *Adv Mater* **2017,** *29* (36).

20. Dutta, G. K.; Han, A. R.; Lee, J.; Kim, Y.; Oh, J. H.; Yang, C., Visible-Near Infrared Absorbing Polymers Containing Thienoisoindigo and Electron-Rich Units for

Organic Transistors with Tunable Polarity. *Advanced Functional Materials* **2013,** *23* (42), 5317-5325.

21. Huang, J.; Chen, Z.; Mao, Z.; Gao, D.; Wei, C.; Lin, Z.; Li, H.; Wang, L.; Zhang, W.; Yu, G., Tuning Frontier Orbital Energetics of Azaisoindigo-Based Polymeric Semiconductors to Enhance the Charge-Transport Properties. *Advanced Electronic Materials* **2017,** *3* (11), 1700078.

22. Wang, F.; Dai, Y.; Wang, W.; Lu, H.; Qiu, L.; Ding, Y.; Zhang, G., Incorporation of Heteroatoms in Conjugated Polymers Backbone toward Air-Stable, High-Performance n-Channel Unencapsulated Polymer Transistors. *Chemistry of Materials* **2018,** *30* (15), 5451-5459.

23. Kang, I.; Yun, H. J.; Chung, D. S.; Kwon, S. K.; Kim, Y. H., Record high hole mobility in polymer semiconductors via side-chain engineering. *J Am Chem Soc* **2013,** *135* (40), 14896-14899.

24. Yao, J.; Yu, C.; Liu, Z.; Luo, H.; Yang, Y.; Zhang, G.; Zhang, D., Significant Improvement of Semiconducting Performance of the Diketopyrrolopyrrole-Quaterthiophene Conjugated Polymer through Side-Chain Engineering via Hydrogen-Bonding. *J Am Chem Soc* **2016,** *138* (1), 173-185.

25. Lin, Y.; Zhao, F.; Prasad, S. K. K.; Chen, J. D.; Cai, W.; Zhang, Q.; Chen, K.; Wu, Y.; Ma, W.; Gao, F.; Tang, J. X.; Wang, C.; You, W.; Hodgkiss, J. M.; Zhan, X., Balanced Partnership between Donor and Acceptor Components in Nonfullerene Organic Solar Cells with >12% Efficiency. *Adv Mater* **2018,** *30* (16), 1706363.

26. Li, W.; Ye, L.; Li, S.; Yao, H.; Ade, H.; Hou, J., A High-Efficiency Organic Solar Cell Enabled by the Strong Intramolecular Electron Push-Pull Effect of the Nonfullerene Acceptor. *Adv Mater* **2018,** *30* (16), 1707170.

27. Zhang, W.; Han, Y.; Zhu, X.; Fei, Z.; Feng, Y.; Treat, N. D.; Faber, H.; Stingelin, N.; McCulloch, I.; Anthopoulos, T. D.; Heeney, M., A Novel Alkylated Indacenodithieno[3,2-b]thiophene-Based Polymer for High-Performance Field-Effect Transistors. *Adv Mater* **2016,** *28* (20), 3922-3927.

28. Liu, Y.; Wang, F.; Chen, J.; Wang, X.; Lu, H.; Qiu, L.; Zhang, G., Improved Transistor Performance of Isoindigo-Based Conjugated Polymers by Chemically

Blending Strongly Electron-Deficient Units with Low Content To Optimize Crystal Structure. *Macromolecules* **2018,** *51* (2), 370-378.

29. Jung, J. W.; Liu, F.; Russell, T. P.; Jo, W. H., Semi-crystalline random conjugated copolymers with panchromatic absorption for highly efficient polymer solar cells. *Energ Environ Sci* **2013,** *6* (11), 3301-3307.

30. Kim, K.-H.; Park, S.; Yu, H.; Kang, H.; Song, I.; Oh, J. H.; Kim, B. J., Determining Optimal Crystallinity of Diketopyrrolopyrrole-Based Terpolymers for Highly Efficient Polymer Solar Cells and Transistors. *Chemistry of Materials* **2014,** *26* (24), 6963-6970.

31. Deng, P.; Wu, B.; Lei, Y. L.; Cao, H. Y.; Ong, B. S., Regioregular and Random Difluorobenzothiadiazole Electron Donor-Acceptor Polymer Semiconductors for Thin-Film Transistors and Polymer Solar Cells. *Macromolecules* **2016,** *49* (7), 2541-2548.

32. Nair, V. S.; Sun, J.; Qi, P.; Yang, S.; Liu, Z.; Zhang, D.; Ajayaghosh, A., Conjugated Random Donor-Acceptor Copolymers of 1 Benzothieno 3,2-b benzothiophene and Diketopyrrolopyrrole Units for High Performance Polymeric Semiconductor Applications. *Macromolecules* **2016,** *49* (17), 6334-6342.

33. Kim, Y.; Cook, S.; Tuladhar, S. M.; Choulis, S. A.; Nelson, J.; Durrant, J. R.; Bradley, D. D. C.; Giles, M.; McCulloch, I.; Ha, C.-S.; Ree, M., A strong regioregularity effect in self-organizing conjugated polymer films and high-efficiency polythiophene:fullerene solar cells. *Nature materials* **2006,** *5* (3), 197-203.

34. Son, S. Y.; Kim, Y.; Lee, J.; Lee, G. Y.; Park, W. T.; Noh, Y. Y.; Park, C. E.; Park, T., High-Field-Effect Mobility of Low-Crystallinity Conjugated Polymers with Localized Aggregates. *Journal of the American Chemical Society* **2016,** *138* (26), 8096-8103.

35. Khim, D.; Cheon, Y. R.; Xu, Y.; Park, W.-T.; Kwon, S.-K.; Noh, Y.-Y.; Kim, Y.-H., Facile Route To Control the Ambipolar Transport in Semiconducting Polymers. *Chemistry of Materials* **2016,** *28* (7), 2287-2294.

36. Burkhart, B.; Khlyabich, P. P.; Thompson, B. C., Influence of the Acceptor Composition on Physical Properties and Solar Cell Performance in Semi-Random

Two-Acceptor Copolymers. *Acs Macro Letters* **2012,** *1* (6), 660-666.

37. Duan, C.; Gao, K.; van Franeker, J. J.; Liu, F.; Wienk, M. M.; Janssen, R. A. J., Toward Practical Useful Polymers for Highly Efficient Solar Cells via a Random Copolymer Approach. *Journal of the American Chemical Society* **2016,** *138* (34), 10782-10785.

38. Kang, T. E.; Kim, K.-H.; Kim, B. J., Design of terpolymers as electron donors for highly efficient polymer solar cells. *Journal of Materials Chemistry A* **2014,** *2* (37), 15252-15267.

39. Jiang, J.-M.; Chen, H.-C.; Lin, H.-K.; Yu, C.-M.; Lan, S.-C.; Liu, C.-M.; Wei, K.-H., Conjugated random copolymers of benzodithiophene-benzooxadiazole-diketopyrrolopyrrole with full visible light absorption for bulk heterojunction solar cells. *Polymer Chemistry* **2013,** *4* (20), 5321-5328.

40. Zhou, J.; Xie, S.; Amond, E. F.; Becker, M. L., Tuning Energy Levels of Low Bandgap Semi-Random Two Acceptor Copolymers. *Macromolecules* **2013,** *46* (9), 3391-3394.

41. Kang, T. E.; Cho, H.-H.; Kim, H. J.; Lee, W.; Kang, H.; Kim, B. J., Importance of Optimal Composition in Random Terpolymer-Based Polymer Solar Cells. *Macromolecules* **2013,** *46* (17), 6806-6813.

42. Li, H.; Liu, F.; Wang, X.; Gu, C.; Wang, P.; Fu, H., Diketopyrrolopyrrole-Thiophene-Benzothiadiazole Random Copolymers: An Effective Strategy To Adjust Thin-Film Crystallinity for Transistor and Photovoltaic Properties. *Macromolecules* **2013,** *46* (23), 9211-9219.

43. Mei, J.; Kim, D. H.; Ayzner, A. L.; Toney, M. F.; Bao, Z., Siloxane-terminated solubilizing side chains: bringing conjugated polymer backbones closer and boosting hole mobilities in thin-film transistors. *J Am Chem Soc* **2011,** *133* (50), 20130-20133.

44. Lei, T.; Dou, J. H.; Pei, J., Influence of alkyl chain branching positions on the hole mobilities of polymer thin-film transistors. *Adv Mater* **2012,** *24* (48), 6457-6461.

45. Zhang, F.; Hu, Y.; Schuettfort, T.; Di, C. A.; Gao, X.; McNeill, C. R.; Thomsen, L.; Mannsfeld, S. C.; Yuan, W.; Sirringhaus, H.; Zhu, D., Critical role of alkyl chain

branching of organic semiconductors in enabling solution-processed N-channel organic thin-film transistors with mobility of up to 3.50 cm(2) V(-1) s(-1). *J Am Chem Soc* **2013,** *135* (6), 2338-2349.

46. Fu, B.; Baltazar, J.; Sankar, A. R.; Chu, P.-H.; Zhang, S.; Collard, D. M.; Reichmanis, E., Enhancing Field-Effect Mobility of Conjugated Polymers Through Rational Design of Branched Side Chains. *Advanced Functional Materials* **2014,** *24* (24), 3734-3744.

47. Back, J. Y.; Yu, H.; Song, I.; Kang, I.; Ahn, H.; Shin, T. J.; Kwon, S.-K.; Oh, J. H.; Kim, Y.-H., Investigation of Structure–Property Relationships in Diketopyrrolopyrrole-Based Polymer Semiconductors via Side-Chain Engineering. *Chem Mater* **2015,** *27* (5), 1732-1739.

48. Fallon, K. J.; Santala, A.; Wijeyasinghe, N.; Manley, E. F.; Goodeal, N.; Leventis, A.; Freeman, D. M. E.; Al-Hashimi, M.; Chen, L. X.; Marks, T. J.; Anthopoulos, T. D.; Bronstein, H., Effect of Alkyl Chain Branching Point on 3D Crystallinity in High N-Type Mobility Indolonaphthyridine Polymers. *Advanced Functional Materials* **2017,** *27* (43), 1704069.

49. Liu, Z.; Zhang, G.; Zhang, D., Modification of Side Chains of Conjugated Molecules and Polymers for Charge Mobility Enhancement and Sensing Functionality. *Accounts of chemical research* **2018,** *51* (6), 1422-1432.

50. Liu, X.; He, B.; Garzón-Ruiz, A.; Navarro, A.; Chen, T. L.; Kolaczkowski, M. A.; Feng, S.; Zhang, L.; Anderson, C. A.; Chen, J.; Liu, Y., Unraveling the Main Chain and Side Chain Effects on Thin Film Morphology and Charge Transport in Quinoidal Conjugated Polymers. *Advanced Functional Materials* **2018,** *28* (31), 1801874.

51. You, H.; Kim, D.; Cho, H.-H.; Lee, C.; Chong, S.; Ahn, N. Y.; Seo, M.; Kim, J.; Kim, F. S.; Kim, B. J., Shift of the Branching Point of the Side-Chain in Naphthalenediimide (NDI)-Based Polymer for Enhanced Electron Mobility and All-Polymer Solar Cell Performance. *Advanced Functional Materials* **2018,** *28* (39), 1803613.

52. Wang, Z.; Liu, Z.; Ning, L.; Xiao, M.; Yi, Y.; Cai, Z.; Sadhanala, A.; Zhang, G.; Chen, W.; Sirringhaus, H.; Zhang, D., Charge Mobility Enhancement for Conjugated

DPP-Selenophene Polymer by Simply Replacing One Bulky Branching Alkyl Chain with Linear One at Each DPP Unit. *Chem Mater* **2018,** *30* (9), 3090-3100.

53. Zheng, Y.-Q.; Wang, Z.; Dou, J.-H.; Zhang, S.-D.; Luo, X.-Y.; Yao, Z.-F.; Wang, J.-Y.; Pei, J., Effect of Halogenation in Isoindigo-Based Polymers on the Phase Separation and Molecular Orientation of Bulk Heterojunction Solar Cells. *Macromolecules* **2015,** *48* (16), 5570-5577.

54. Yan, Z.; Sun, B.; Li, Y., Novel stable (3E,7E)-3,7-bis(2-oxoindolin-3-ylidene)benzo[1,2-b:4,5-b′]difuran-2,6(3H,7H)-dione based donor–acceptor polymer semiconductors for n-type organic thin film transistors. *Chemical Communications* **2013,** *49* (36), 3790.

55. Zhang, G.; Li, P.; Tang, L.; Ma, J.; Wang, X.; Lu, H.; Kang, B.; Cho, K.; Qiu, L., A bis(2-oxoindolin-3-ylidene)-benzodifuran-dione containing copolymer for high-mobility ambipolar transistors. *Chemical Communications* **2014,** *50* (24), 3180.

56. Lei, T.; Dou, J. H.; Cao, X. Y.; Wang, J. Y.; Pei, J., A BDOPV-based donor-acceptor polymer for high-performance n-type and oxygen-doped ambipolar field-effect transistors. *Adv Mater* **2013,** *25* (45), 6589-6593.

57. Zhang, G.; Fu, Y.; Xie, Z.; Zhang, Q., Synthesis and Photovoltaic Properties of New Low Bandgap Isoindigo-Based Conjugated Polymers. *Macromolecules* **2011,** *44* (6), 1414-1420.

58. Ge, F.; Wei, S.; Liu, Z.; Wang, G.; Wang, X.; Zhang, G.; Lu, H.; Cho, K.; Qiu, L., Tailoring Structure and Field-Effect Characteristics of Ultrathin Conjugated Polymer Films via Phase Separation. *ACS Appl Mater Interfaces* **2018,** *10* (11), 9602-9611.

59. Donley, C. L.; Zaumseil, J.; Andreasen, J. W.; Nielsen, M. M.; Sirringhaus, H.; Friend, R. H.; Kim, J. S., Effects of Packing Structure on The Optoelectronic And Charge Transport Properties in Poly(9,9-di-n-octylfluorene-alt-benzothiadiazole). *J. Am. Chem. Soc.* **2005,** *127*, 12890-12899.